Calculation of the effective interaction parameter in the LDA+U method by a linear response approach for $Fe(OH)_2$

Mansoureh Pashangpour,[1] Amir Abbas Sabouri-Dodaran,[2,3] Khadijeh Imani,[4] and Nasser Nafari[5]
[1]*Science and Research Branch, Islamic Azad University, Tehran 14155-4933, Iran*
[2]*Payame Noor University, Tehran 19395-4697, Iran*
[3]*The Abdus Salam International Centre for Theoretical Physics (ICTP), 34014 Trieste, Italy*
[4]*Islamic Azad University, Karaj Branch, Tehran 31485-313, Iran*
[5]*Institute for Theoretical Physics and Mathematics, Tehran 19395-5531, Iran*
(Received 15 January 2009; revised manuscript received 15 August 2009; published 6 October 2009)

In this paper we have investigated the electronic properties of $Fe(OH)_2$ hydroxide by using the spin-polarized version of the generalized gradient approximation (σ-GGA) as well as the σ-GGA+U. Our calculations for the iron hydroxide show that the σ-GGA results are at variance with experimental findings. On the other hand, we have shown that σ-GGA+U is capable of opening a gap at the Fermi level resulting in an insulating ground state. Moreover, the frequencies of the Raman-active A_{1g}(OH) and infrared-active A_{2u}(OH) stretching modes of OH group are calculated at ambient conditions. We have found the calculated gap as well as the calculated frequencies are in good agreement with experimental results.

DOI: 10.1103/PhysRevB.80.155111 PACS number(s): 71.15.Mb, 71.15.Nc, 71.20.−b

I. INTRODUCTION

Several authors have investigated the electronic properties of layered hydroxides. In particular, brucite-type hydroxides with the general formula $M^{2+}(OH)_2$, where M^{2+} stands for a divalent cation, are extensively studied. The study of the electronic structure of these materials as well as the study of their temperature-pressure phase diagram has helped the physicists to gain a better understanding of the Earth's crust and mantel. It is well known that these hydroxides are abundantly found on the Earth's surface. In this paper we have concentrated on the electronic structure of the hydroxide $Fe(OH)_2$, commonly known as white rust, and in particular, we have addressed its insulating phase by studying its band structure. $Fe(OH)_2$ has a hexagonal crystal structure and is isostructural with brucites, $Mg(OH)_2$, $Ca(OH)_2$, $Mn(OH)_2$, β-$Co(OH)_2$, and β-$Ni(OH)_2$. Factor group analysis at the Brillouin-zone center determines that there are two internal stretching OH vibrations, i.e., the symmetric A_{1g}(OH), the antisymmetric A_{2u}(OH) modes, and six lattice modes A_{1g}(T), A_{2u}(T), E_g(T), E_u(T), E_g(R), and E_u(R).[1]

Both the local spin-density approximation (LSDA) and the spin-polarized version of the generalized gradient approximation (σ-GGA) fail to predict the insulating behavior of $Fe(OH)_2$. It is known that the transition-metal oxides encounter a similar problem.[2] But the LDA+U approach which was first introduced by Anisimov *et al.*,[3] and its variants such as LSDA+U or σ-GGA+U, allow us to study some of the properties of the strongly correlated electron systems, with considerable improvement over the LSDA or σ-GGA results. In fact, the standard density-functional theory (DFT) within the framework of Kohn-Sham formalism which employs LSDA or σ-GGA predicts an unphysical metallic character for $Fe(OH)_2$. This is due to the fact that the crystal field and the electronic-structure effects are not sufficient in this case to open a gap at the Fermi level. As expected, we have shown that the LSDA+U and σ-GGA+U schemes predict the insulating behavior of $Fe(OH)_2$ with a gap close to the experimental findings.[4]

The organization of this paper is as follows. In Sec. II we present the σ-GGA+U approach which starts with the formulation of Anisimov *et al.*[2,5–8] We have employed this formulation for the LSDA+U and σ-GGA+U schemes, where the evaluation of the interaction parameters is based on the linear-response theory.[9] In Sec. III, the computational details are described. In Sec. IV the application of this methodology for studying the electronic properties of $Fe(OH)_2$ as a strongly correlated system is discussed. Moreover, the frequencies of the Raman-active and infrared-active stretching modes of OH, as well as the magnetic moment of Fe^{2+} in $Fe(OH)_2$ are evaluated. Finally, in Sec. V the concluding remarks are presented.

II. THEORETICAL DETAILS

Anisimov *et al.* have extended the standard local-density approximation (LDA) employed in DFT to the LDA+U by adding an on-site Hubbard-type interaction E_{Hub}. This term accounts for the on-site Coulomb interaction and is responsible for the correlation gap occurring in Mott insulators.[5] The suggested energy functional has the following form:

$$E_{\mathrm{LDA}+U}[n(\mathbf{r})] = E_{\mathrm{LDA}}[n(\mathbf{r})] + E_{\mathrm{Hub}}[\{n^{I\sigma}_{mm'}\}] - E_{DC}[\{n^{I\sigma}\}], \tag{1}$$

where $n(\mathbf{r})$ is the electronic density and $n^{I\sigma}_{mm'}$ are the atomic-orbital occupations for the atom I with spin σ. The last term in this equation is to avoid double counting of the interactions contained in E_{Hub}, and in some averaged way, in E_{LDA}. The E_{DC} term represents the mean-field approximation to the LDA contribution of on-site electronic interactions. In this term, $n^{I\sigma}$ is the trace of $n^{I\sigma}_{mm'}$ over magnetic quantum number m. A rotationally invariant formulation has been introduced[2,8] where the orbital dependence of E_{Hub} is defined by Eq. (2) in Ref. 9.

In this procedure we introduce the response functions as the localized level occupations with respect to the potential

shift in d levels. By using the response-function approach,[9,10] the effective interaction parameter U is deduced from the following equations:

$$\chi_{IJ} = \frac{dn_d^I}{d\alpha_J}, \tag{2}$$

$$U = -\frac{d\alpha_I}{dn_d^I} + \frac{d\alpha_I}{dn_{d0}^I} = (\chi_0^{-1} - \chi^{-1})_{II}. \tag{3}$$

Here χ_{IJ} are the elements of the linear response matrix, n_d^I is the occupation number of the d levels and α_I represents the potential shift. χ (the screened response matrix) includes all screening effects from crystal environment which is associated with the localized electrons and χ_0 (the unscreened response matrix) contains nonscreening effects of the total energy of the noninteracting Kohn-Sham qausiparticles associated with the system. Therefore, for eliminating the nonscreening effects in the evaluation of the physical value of U, χ_0^{-1} must be subtracted from χ^{-1}. To compute the Hubbard effective interaction U, we used LSDA calculations with potential shift acting on the d levels in one of the Hubbard atoms which in this case are the iron sites. For evaluating the on-site Coulomb interaction U, we only considered the nearest-neighbor electronic interactions of iron sites and in our numerical calculations we used two supercells with different number of iron atoms. We performed a series of perturbations on Hubbard atoms (iron atoms). Moreover, we considered a delocalized background which adds one more column and one more row to the response matrix. These elements are determined by imposing overall charge neutrality of the perturbed system for all localized perturbations

$$\sum_I \chi_{IJ} = 0, \quad \sum_I \chi_{IJ}^0 = 0, \quad \text{for all } J, \tag{4}$$

$$\sum_J \chi_{IJ} = 0, \quad \sum_J \chi_{IJ}^0 = 0, \quad \text{for all } I. \tag{5}$$

It is worth mentioning that the singularities in χ^{-1} and χ_0^{-1} can be avoided when computing the difference $\chi_0^{-1} - \chi^{-1}$ by shifting the elements of χ_0 and χ matrices with the same amount.

III. COMPUTATIONAL DETAILS

Our calculations are based on the use of DFT and the *ab initio* pseudopotential plane-wave method using the PWSCF code of the Quantum ESPRESSO distribution.[11] We start our calculations with a hexagonal unit cell (space group $p\bar{3}m1$) and assume that the hydroxide $Fe(OH)_2$ is in its antiferromagnetic structure with the magnetic moments aligned in the basal plane. Fe atoms are located at (0, 0, 0) and (0, 0, 0.5). The O and H atoms are located at (1/3, 2/3, z), (1/3, 2/3, z +0.5), (2/3, 1/3, 0.5−z), and (2/3, 1/3, 1−z) with $z \sim 0.1$ for O atoms and $z \sim 0.2$ for H atoms. All coordinate numbers are specified in crystal units. Experimental lattice parameters are $a=6.166$ a.u. and $c=17.399$ a.u.[12–14] Note that the z values reported by Lutz *et al.*[14] ($z=0.22$ for O atoms and $z=0.44$ for H atoms) are almost two times greater than ours. This is because the c-cell parameter of our super cell is two times greater than theirs. Thus, the two sets of z values along with their c parameters are compatible and their small differences are due to the use of the geometry relaxation in our case and the use of the experimental results in theirs.

The calculations are performed with the ultrasoft GGA Perdew-Burke-Ernzerhof (U.S. PBE) (Ref. 15) nonlinear core-correction (NLCC) pseudopotential for iron atoms while for oxygen and hydrogen U.S. PBE (non-NLCC) pseudopotentials have been chosen. We also performed the calculations with U.S. LDA Perdew-Zunger (PZ) (Ref. 16) NLCC for iron atoms and U.S. PZ (non-NLCC) pseudopotentials for oxygen and hydrogen. For the pseudopotential generation we used the $3d^7 4s^1$ valence-atomic-orbital configuration for iron, the $2s^2 2p^4$ for oxygen and the $1s^1$ for hydrogen. Brillouin-Zone integrations were performed using $6\times6\times3$ Monkhorst and Pack[17] special point grids using Marzari and Vanderbilt smearing technique with a smearing width of 0.008 Ry in order to smooth the Fermi distribution. The Kohn-Sham orbitals are expanded in a plane-wave-basis set. The energy cut off for the wave function and the charge density are respectively 50 and 400 Ry. These values are used because of the ultrasoft pseudopotentials for Fe, O, and H and the imposed periodic boundary conditions. The optimized lattice parameters of $Fe(OH)_2$ after relaxation are: $a=6.105$ a.u., $c=17.396$ a.u., and $z=0.115$ for O atoms and $z=0.221$ for H atoms expressed in crystal unit. After performing the optimization, we have found that the optimized volume is 2% less than the experimental results.[13] In order to compute the Hubbard interaction U, we have used potential shifting which acts on the iron ion to study the response of the d atomic occupations on the perturbed site and on the other atoms in the system. For this purpose, we performed a series of self-consistent calculations with different potential shifts in the d levels of one of the iron ions. Then, through Eqs. (2) and (3), we obtained the response matrices χ and χ^0. The perturbed atom, with a shifted potential in the d channel, strongly interacts with its nearest neighbors. This screening process is not completely efficient. Thus, we performed perturbation in a larger supercell to consider the nearest-neighbors contribution in the response matrices. First, we considered C1 supercell with two iron ions and then extrapolated the result to C4 supercell which contains four C1 supercells with eight iron ions (See Fig. 1).

IV. RESULTS AND DISCUSSION; FOR DIFFERENT SUPERCELLS

A. C1 supercell

The C1 supercell contains two iron atoms in a hexagonal structure with opposite spin polarizations [Fe1 and Fe2 in Fig. 1(a)]. Figure 2 shows the variation in d-level occupation of Fe ions in terms of potential shifts in the first iteration of perturbation when the perturbed atom is Fe1. In this manner the nonscreening part of linear response χ_0 is defined. For the purpose of clarification, we mention that the density response obtained at the first iteration does not involve any effect of the electron-electron interaction and, in fact, it cor-

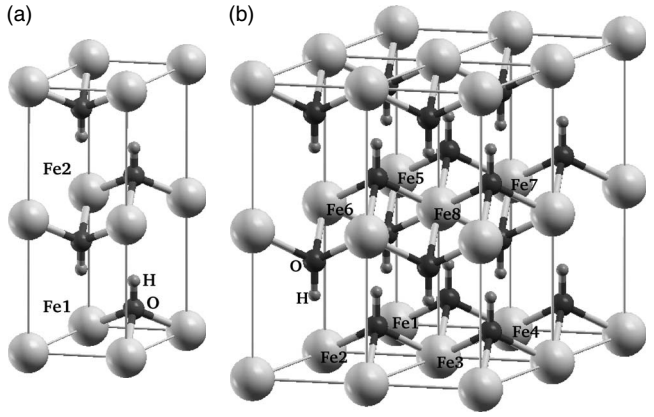

FIG. 1. (a) C1 supercell with opposite spin polarization for the two iron atoms, Fe1 and Fe2, and (b) C4 supercell with eight iron atoms.

responds to the response of the independent electron system. The slopes of the two lines in Fig. 2 are −1.2464 Ry^{-1} and 1.0634 Ry^{-1}, but if the perturbed atom is Fe2, these slopes are slightly shifted relative to the previous result. In this way we obtain the elements of the nonscreening linear response matrix, i.e., χ^0_{11}, χ^0_{12}, χ^0_{21}, and χ^0_{22}.

After repeating the iteration cycle for sufficient number of times, i.e., after the electron-electron interaction has fully played its role, we obtain the screened linear response χ matrix which, in turn, via Eq. (3) results in the evaluation of the Hubbard interaction parameter U. Figure 3 shows the variations in d-levels occupation of Fe ions in terms of potential shifts in the last iteration of perturbation when the perturbed atom is Fe1. The slopes of the lines in Fig. 3 are −0.1460 Ry^{-1} and 0.0181 Ry^{-1}. We obtain a similar figure when the perturbed atom is Fe2. In this case the slopes are 0.0179 Ry^{-1} and −0.1457 Ry^{-1}.

In order to avoid the singularities in χ^{-1} and χ_0^{-1}, appearing in Eq. (3), one adds the delocalized background to both χ and χ_0. Diagonal elements of $\chi_0^{-1}-\chi^{-1}$ show the value of the effective interaction parameter for C1 supercell as 2.96 eV and nondiagonal terms correspond to the intersite effective interaction in the local-density approximation.

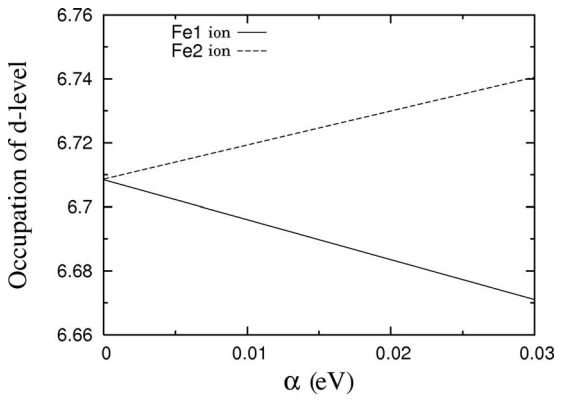

FIG. 2. Occupation of d levels of Fe ions as a function of potential shift, α, on Fe1 ion in the first iteration of perturbation. This gives the independent electron system response χ_0.

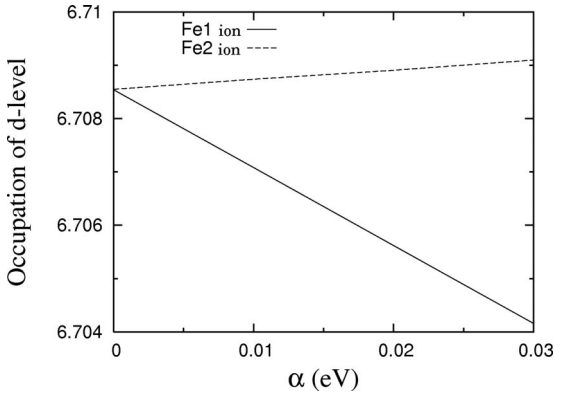

FIG. 3. Occupation of d levels of Fe ions as a function of the potential shift, α, on Fe1 ion in the final iteration of perturbation using the fully screened response, when Fe1 in supercell C1 is perturbed.

B. C4 supercell

The results obtained using the C1 supercell can be corrected by considering a larger supercell, i.e., the C4 supercell with eight iron ions in the unit cell [Fig. 1(b)]. By considering the nearest-neighbors contribution, the effective interaction can be estimated more efficiently. Thus, in order to obtain the response functions, we first perturb the potential on the d levels of one particular iron ion in the C4 supercell. The results are shown in Fig. 4. According to Fig. 4(a), the slopes of the lines are 0.5129 Ry^{-1}, −2.998 Ry^{-1}, 0.3246 Ry^{-1}, and 0.3244 Ry^{-1} and the value of these slopes in Fig. 4(b), when the perturbed ion is Fe2 in C4 supercell, are 0.0168 Ry^{-1}, −0.1949 Ry^{-1}, 0.0048 Ry^{-1}, and 0.0057 Ry^{-1}. We note that the C4 supercell gives rise slightly to a larger U value. This is due to the fact that the effect of nearest-neighbors' contributions in the value of U is positive (See Ref. 8). So, we expect the calculated U value for C1-supercell turn out to be less than the U value for C4 supercell.

By considering the background effects in χ and χ^0 response matrices, the diagonal elements of the matrix $\chi_0^{-1}-\chi^{-1}$ gives us the value of the Hubbard U on the iron sites in C4 supercell. The result is U=4.05 eV. The C4 supercell is believed to be large enough to compute the Hubbard U for Fe atoms in $Fe(OH)_2$. So, the calculation for a somewhat larger supercell results in a negligible change in our U value. As a result, we have used this computed interaction parameter in our LSDA+U and σ-GGA+U calculations to obtain some of the physical properties of this compound. In order to obtain the d-level occupation numbers more accurately whenever necessary, we have used localized Wannier functions of the bands around the Fermi energy. Figure 5 demonstrates the change in the total density of states for the bulk $Fe(OH)_2$ considering the on-site effective Coulomb interaction U in the two cases of 0 and 4.05 eV. The energy of the Fermi level is set to zero. By taking into account the on-site correlation effects, Fe-d bands below/above the Fermi level are shifted to a lower/higher energy level which results in a notable gap.

Apart from the change in the density of states, one can observe that there are changes of the projected density of

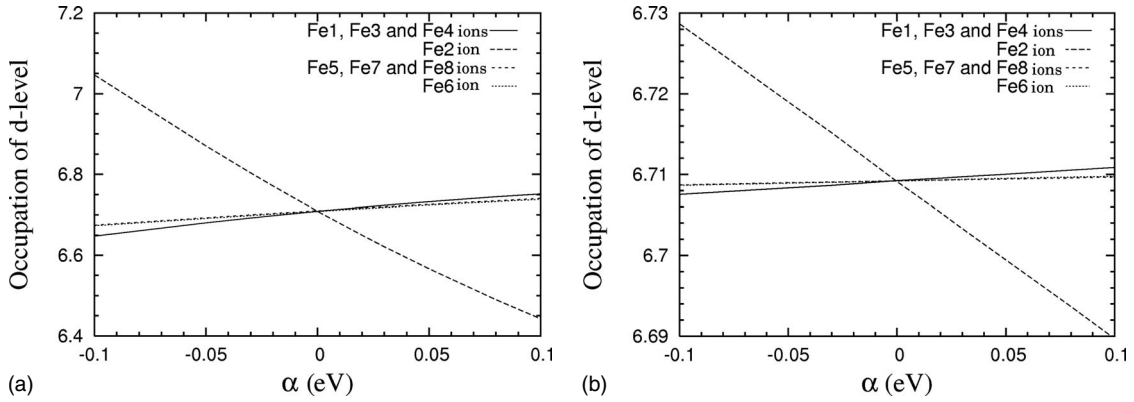

FIG. 4. Occupation of d levels of iron ions in terms of the potential shift, α, on Fe2 ion for C4 supercell; (a) in the first iteration of perturbation (nonscreening part of linear response, χ_0), (b) in the final iteration of perturbation (fully screened part of linear response, χ).

states (PDOS) weights near the Fermi level (See Fig. 6). Fe-3d orbital are split into $e_g^{(1)}$ and t_{2g} states by the crystal field with octahedral symmetry. The measured bond lengths surrounding a given Fe atom are 3.253 Å and 2.827 Å, and the bond angles formed by Fe and O atoms are 98° and 82° (See Ref. 1). The crystal field of this distorted (compressed) octahedron has D_{3d} point-group symmetry. According to the group representation of D_{3d} the triplet t_{2g} level splits into a doublet, $e_g^{(2)}$, and a singlet a_{1g}. Consequently, we end up with a singlet, a_{1g}, and two doublets, $e_g^{(1)}$, $e_g^{(2)}$. By calculating the d-orbital occupation numbers and in accordance with the Hund's first rule, we have found that all majority (spin-up) states and the a_{1g} minority (spin-down) state are occupied. Moreover, as Fig. 6 shows, our calculated d-orbital occupation numbers are in agreement with our PDOS results where the a_{1g} minority state lies below the Fermi level and the two doublet minority states lie above the Fermi level. Since the minority a_{1g} (spin-down) state becomes occupied, the symmetry would not be further lowered. The result is compatible with the work of Sams *et al.*[18] for a compression along the quantization axis presented in their discussion section.

As a result within the σ-GGA+U and due to the gap opening the minority-spin states of the t_{2g} manifold of iron are split into two subgroups. Within σ-GGA+U the lower energy minority-spin d-state merge in the group of states below the Fermi level where it mixes strongly with the states originating from oxygen p orbital and majority-spin d-states of the iron ions.

The calculated band structure of $Fe(OH)_2$ using σ-GGA +U with U=4.05 eV is shown in Fig. 7(b). We obtain the insulating behavior which is deduced from the band structure shown in Fig. 7(b). As this figure shows a gap opens around the Fermi level with a minimal width of about 2.29 ± 0.05 eV. This band gap now separates the valence band from the conduction band. This is in contrast to the case of σ-GGA with metallic band structure [See Fig. 7(a)]. The obtained band-gap value is in good agreement with the experimental optical band gap which is 2.1 ± 0.05 eV.[4] The band gap is direct and located at the Γ point. Moreover, from the σ-GGA band-structure calculation it is seen that the band width, W, is 0.86 eV, resulting in the ratio of $U/W \approx 4.71$. The value of this ratio indicates that the hydroxide $Fe(OH)_2$ belongs to the strongly correlated electron system.

We also considered the following two transitions, (i) $\{3d(\mathrm{Fe}), 2p(\mathrm{O})\} \rightarrow 4s(\mathrm{Fe})$ and (ii) $\{3d(\mathrm{Fe}), 2p(\mathrm{O})\} \rightarrow 3d(\mathrm{Fe})$. These transitions are of interest in an optical band-gap measurement of $Fe(OH)_2$ hydroxide. First, we show that both of these transitions satisfy the dipole selection rules and second we present the results obtained via σ-GGA+U. In the case of an isolated atom interacting with light, the dipole selection rules takes the following form:

$$\langle n'l', m' | \frac{e}{mc} \mathbf{A} \cdot \mathbf{P} | nl, m \rangle \neq 0,$$

$$\text{when } \Delta l = \pm 1 \text{ and } \Delta \mathrm{m} = -1, 0, 1, \tag{6}$$

where $\mathbf{A}$ is the vector potential, $\mathbf{P} = -i\hbar\vec{\nabla}$ is the momentum operator, and the atomic states $|n'l'm'\rangle$ have the same center. However, in a solid, we have hybridized atomic orbitals centered at different points. Since the matrix elements $\langle d_{\mathrm{Fe}}, p_{\mathrm{O}} | \mathbf{A} \cdot \mathbf{P} | s_{\mathrm{Fe}} \rangle$ and $\langle d_{\mathrm{Fe}}, p_{\mathrm{O}} | \mathbf{A} \cdot \mathbf{P} | d_{\mathrm{Fe}} \rangle$ assume nonzero val-

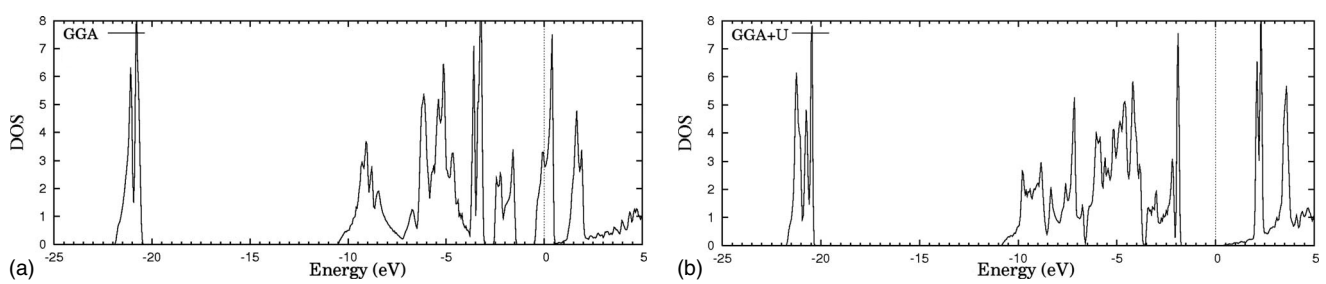

FIG. 5. Density of states of $Fe(OH)_2$ as a function of energy with (a) GGA and (b) σ-GGA+U (U=4.05 eV).

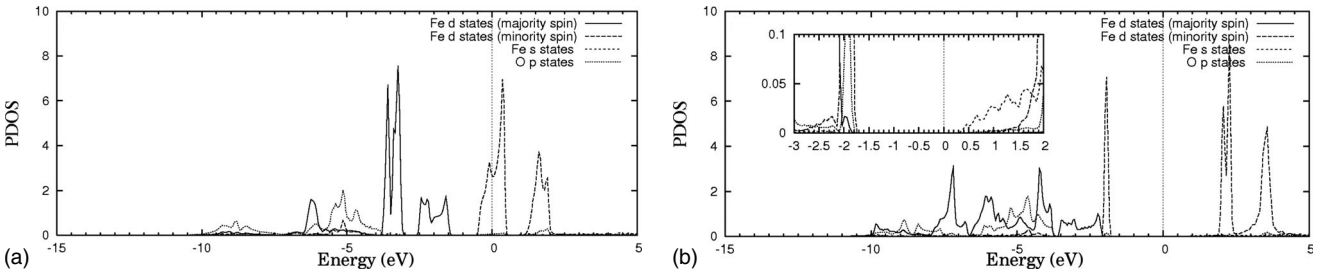

FIG. 6. The projected density of states of $Fe(OH)_2$ as a function of energy with (a) σ-GGA and (b) σ-GGA+U (U=4.05 eV).

ues, both transitions are allowed. The state $|d_{Fe}, p_O\rangle$ is a hybrid state. Our results show that the first transition is predicted to occur at 2.29 ± 0.05 eV and the second transition is predicted to occur at 2.67 ± 0.05 eV within σ-GGA+U [See Fig. 7(b)], and the corresponding values within LSDA+U are, respectively, 1.9 ± 0.05 eV and 2.16 ± 0.05 eV (not shown in here). These results are consistent with our PDOS calculations. From PDOS calculations shown in Fig. 6(b), it is clear that the first transition $\{[3d(\mathrm{Fe}), 2p(\mathrm{O})] \rightarrow 4s(\mathrm{Fe})\}$ is weaker than the second transition $\{[3d(\mathrm{Fe}), 2p(\mathrm{O})] \rightarrow 3d(\mathrm{Fe})\}$. It is known that LSDA and thereby LSDA+U works better for inhomogeneous electron systems with nearly uniform density and usually underestimates the energies. On the other hand, when the electron-density variation is large, one expects the σ-GGA+U to work better than LSDA+U. However, for an intermediate density variation such as ours [$Fe(OH)_2$], it is not clear, at the outset, which one of these two approximations (LSDA or σ-GGA) generates results leading to better agreement with experiments and it is not necessarily the case to observe similar improvements of one approximation over the other for all physical quantities.[19] In fact, our band-gap calculations based on the use of σ-GGA+U leads to a closer agreement with experimental results relative to the LSDA+U, whereas the phonon-frequency calculations based on the σ-GGA leads to an overestimation relative to the LSDA+U. In what follows we will discuss this point in more detail.

We also have performed DFT calculations for the two internal stretching OH vibrations, A_{1g}(OH) and A_{2u}(OH). Using the initial experimental structure, the frequencies of Raman- and infrared-active stretching modes of OH are calculated with ion relaxation (See Table I). By including U in ion relaxation process, i.e., by employing LSDA+U, we found that the calculated frequencies of the A_{1g}(OH) and A_{2u}(OH) phonon modes are in good agreement with the experimental values.[1,13,14,20] Note that the maximum difference between the theoretical and experimental results is about 3% and such a difference is mainly due to the kind of energy functional used in DFT.

The experimental value for the magnetic moment of Fe^{2+} in $Fe(OH_{0.86}D_{0.14})_2$ is $3.50(7)\mu_B$. $Fe(OH_{0.86}D_{0.14})_2$ is structurally and magnetically very similar to the $Fe(OH)_2$.[12] The magnetic moment of Fe^{2+} in $Fe(OH)_2$ is found to be $3.98\mu_B$ using σ-GGA+U calculations with U=4.05 eV.

V. CONCLUDING REMARKS

In this work we have investigated the electronic structure of $Fe(OH)_2$ hydroxide using σ-GGA+U formulation and have employed a method that is based on the linear-response approach to calculate the interaction parameter (Hubbard U) entering the effective potential of the Kohn-Sham formalism in DFT. By this approach we obtained U=4.05 eV. The calculated band structure of this compound within the σ-GGA+U approach shows a gap around the Fermi level whose minimal width is 2.29 ± 0.05 eV. The band gap is direct and is located at the Γ point. It corresponds to the weak transition of $\{3d(\mathrm{Fe}), 2p(\mathrm{O})\} \rightarrow 4s(\mathrm{Fe})$ character at 2.29 ± 0.05 eV and the stronger transition of $\{3d(\mathrm{Fe}), 2p(\mathrm{O})\} \rightarrow 3d(\mathrm{Fe})$ character around 2.67 ± 0.05 eV. Using the band structures within σ-GGA and σ-GGA+U show the ratio of U/W to be 4.71. In LSDA+U calculations the magnetic moment of Fe^{2+} in $Fe(OH)_2$ is $3.98\mu_B$. We have carried out of the frequencies of Raman- and infrared-active stretching modes of OH are carried out with ion relaxation using the experimental cell pa-

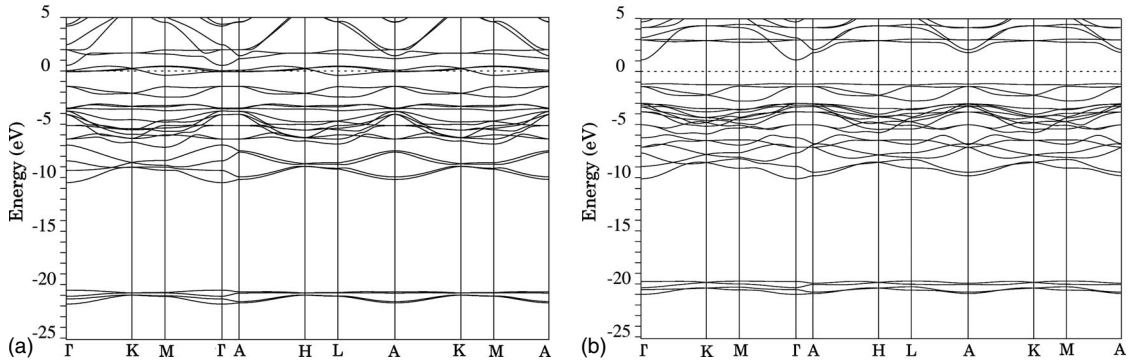

FIG. 7. The band structure for $Fe(OH)_2$ with (a) σ-GGA and (b) σ-GGA+U (U=4.05 eV).

TABLE I. The Raman- and infrared-active stretching modes of OH (in cm^{-1}) for $Fe(OH)_2$ at ambient conditions.

	A_{1g}(OH)	A_{2u}(OH)
σ-GGA	3683.0	3716.7
σ-GGA [a]	3679.4	3711.8
LSDA	3574.8	3605.4
LSDA[b]	3583.1	3620.1
Exp.	3576	3624[c]
	3572 ± 3	3627 ± 1 [d]

[a]With ion relaxation by σ-GGA+U (U=4.05 eV).
[b]With ion relaxation by LSDA+U (U=4.05 eV).
[c]Reference 14.
[d]Reference 1.

rameters and have found good agreement between theory and experiment.

Finally, in our calculation we have only focused on the on-site Coulomb energy U and neglected the exchange interaction, J, defined in Eq. (4) of Ref. 9. In other words, we have set $J=0$. In order to account for the exchange interaction in an approximate manner, one defines an effective on-site Coulomb interaction $U_{eff}=U-J$.[21] However, for strongly correlated electron systems such as $Fe(OH)_2$, where $U \gg J$, neglecting J in U_{eff} is considered to be a reasonable approximation. Moreover, considering the fact that slightly smaller U_{eff} leads to slightly smaller gap, we believe that the inclusion of the exchange interaction parameter would result in a better agreement between the calculations based on the U_{eff} and the experimental gap of Ref. 4. In our future work, we plan to evaluate the J value numerically and repeat our band-structure calculations for the transition-metal hydroxides.

ACKNOWLEDGMENTS

One of us (A.A.S.-D.) would like to thank S. Scandolo and S. de Gironcoli for their valuable discussions. We would also like to thank the anonymous referee for making an interesting comment. This work has been supported by Payame-Noor university and the Computational Nanotechnology Supercomputing Centre, Institute for Research in fundamental Sciences (IPM) Tehran, Iran.

[1] S. Speziale, R. Jeanloz, A. Milner, M. P. Pasternak, and J. M. Zaug, Phys. Rev. B **71**, 184106 (2005).
[2] V. I. Anisimov, F. Aryasetiawan, and A. I. Lieechtenstein, J. Phys.: Condens. Matter **9**, 767 (1997).
[3] V. I. Anisimov and O. Gunnarsson, Phys. Rev. B **43**, 7570 (1991).
[4] F. Di Quarto, M. C. Romano, M. Santamaria, S. Piazza, and C. Sunseri, Russ. J. Electrochem. **36** (11), 1208 (2000).
[5] V. I. Anisimov, J. Zaanen, and O. K. Andersen, Phys. Rev. B **44**, 943 (1991).
[6] V. I. Anisimov, I. V. Solovyev, M. A. Korotin, M. T. Czyzyk, and G. A. Sawatzky, Phys. Rev. B **48**, 16929 (1993).
[7] I. V. Solovyev, P. H. Dederichs, and V. I. Anisimov, Phys. Rev. B **50**, 16861 (1994).
[8] A. I. Liechtenstein, V. I. Anisimov, and J. Zaanen, Phys. Rev. B **52**, R5467 (1995).
[9] M. Cococcioni and S. de Gironcoli, Phys. Rev. B **71**, 035105 (2005).
[10] W. E. Pickett, S. C. Erwin, and E. C. Ethridge, Phys. Rev. B **58**, 1201 (1998).
[11] S. Baroni, A. Dal Corso, S. de Gironocoli, and P. Giannozzi, http://www.pwscf.org and http://www.quantum-espresso.org
[12] J. B. Parise, W. G. Marshall, R. I. Smith, H. D. Lutz, and H. Moller, Am. Mineral. **85**, 189 (2000).
[13] S. H. Shim, S. Rekhi, M. C. Martin, and R. Jeanloz, Phys. Rev. B **74**, 024107 (2006).
[14] H. D. Lutz, H. Moller, and M. Schmidt, J. Mol. Struct. **328**, 121 (1994).
[15] J. P. Perdew, K. Burke, and M. Ernzerhof, Phys. Rev. Lett. **77**, 3865 (1996).
[16] J. P. Perdew and A. Zunger, Phys. Rev. B **23**, 5048 (1981).
[17] H. J. Monkhorst and J. D. Pack, Phys. Rev. B **13**, 5188 (1976).
[18] J. R. Sams, R. C. Thompson, and T. B. Tsin, Can. J. Chem. **55**, 115 (1977).
[19] R. O. Jones and O. Gunnarsson, Rev. Mod. Phys. **61**, 689 (1989).
[20] S. R. Shieh and T. S. Duffy, Phys. Rev. B **66**, 134301 (2002).
[21] S. L. Dudarev, G. A. Botton, S. Y. Savrasov, C. J. Humphreys, and A. P. Sutton, Phys. Rev. B **57**, 1505 (1998).